# Large-Eddy Simulations of Flow over Double-Ridge Orography

Brigitta Goger[1,2], Stefano Serafin[1], Ivana Stiperski[2] and Vanda Grubišić[1,3]

[1] Department of Meteorology and Geophysics, University of Vienna, Vienna (Austria)
[2] Institute of Meteorology and Geophysics, University of Innsbruck, Innsbruck (Austria)
[3] Earth Observing Laboratory, National Center for Atmospheric Research, Boulder (Colorado)

**Poster Z65, Abstract EGU2014-5500**
**Presented at EGU General Assembly 2014, Vienna**

## Introduction

- Flow over a mountain results in **vertical displacements of air parcels**.
- Numerical 2D simulations conducted by Vosper (2004) suggest that the **inversion strength (Δθ)** and **inversion height** ($z_i$) influence the formation of **lee waves** (fig 2), **rotors** (fig 2) and **hydraulic jumps** (fig 3).
- A **regime diagram** (fig 4) describing the occurrence of lee wave rotors or hydraulic jumps is introduced.

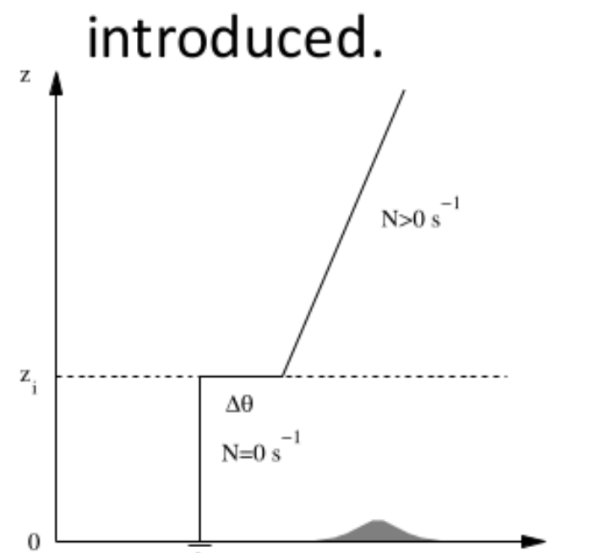

(fig 1) Schematic diagram of the atmospheric profile (Vosper, 2004)

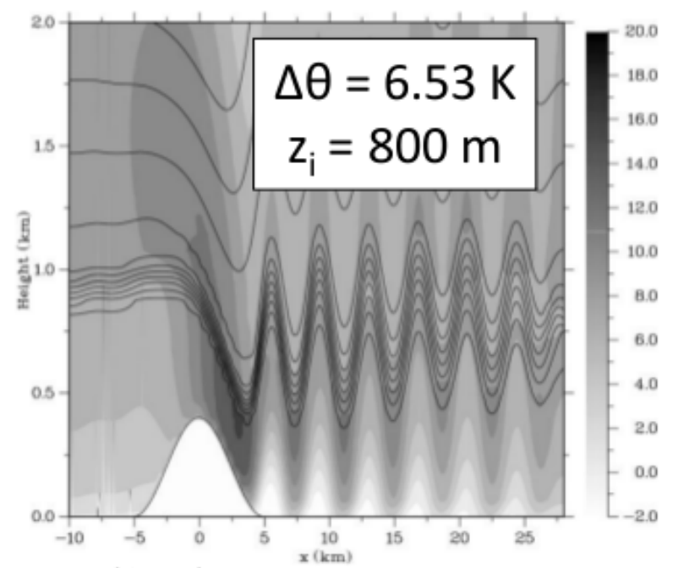

(fig 2) Lee waves and rotors (Vosper, 2004)

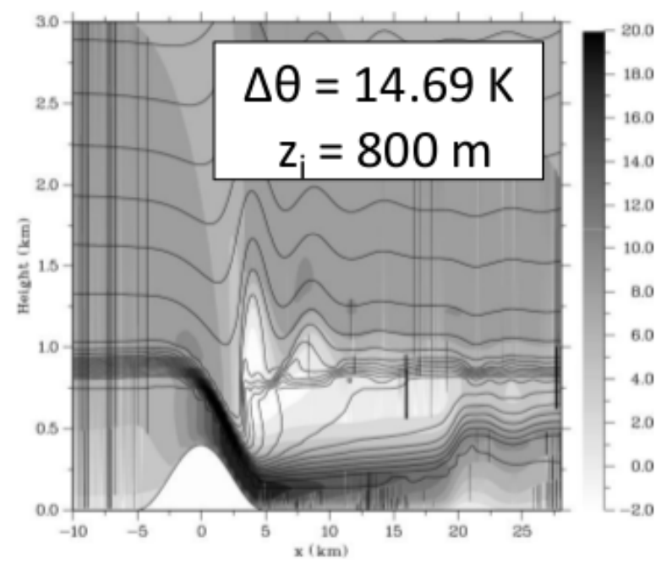

(fig 3) Hydraulic jump (Vosper, 2004)

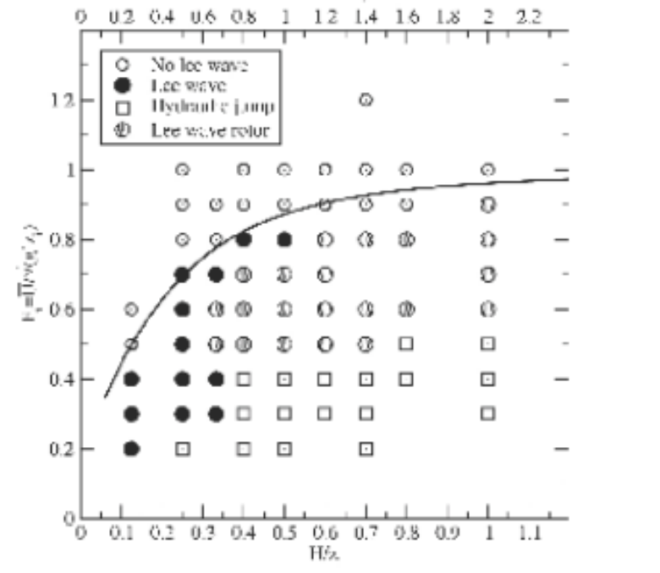

(fig 4) Regime diagram (Vosper, 2004)

### Laboratory experiments

- Laboratory experiments on mountain waves and rotors were carried out by Knigge et al. (2010) in the fluid dynamical facilities CNRM-GAME of Météo France in Toulouse.
- Comparability with the atmospheric equivalents is given by the use of **non-dimensional parameters**.
- By **towing an obstacle** through a water tank, lee wave rotors (fig 5) and hydraulic jumps (fig 6) were observed.

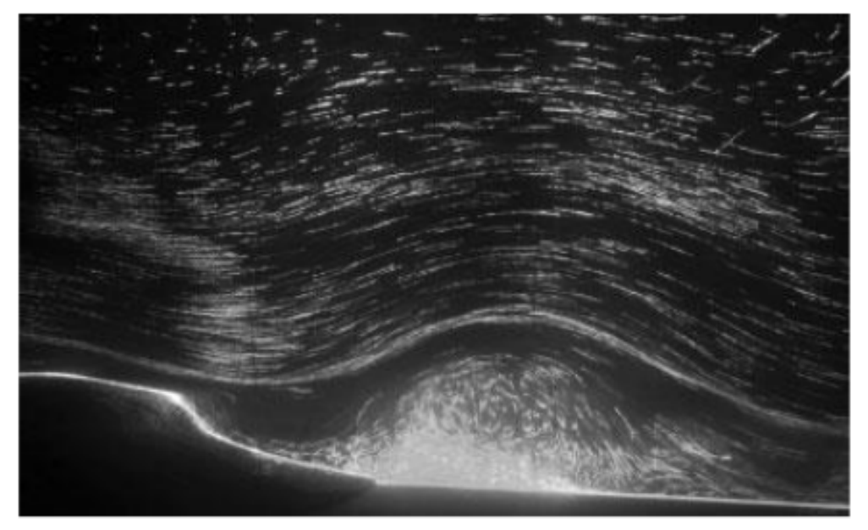

(fig 5) a lee wave rotor in the laboratory (Knigge et al., 2010)

(fig 6) a hydraulic jump in the laboratory (Knigge et al., 2010)

**Non-dimensional parameters**
Mountain/inversion height ratio: $\mathbf{h/z_i}$
Shallow-water Froude number:
$\mathbf{Fr=u/\sqrt{g' z_i}}$

## Influence of a Second Mountain

- Numerical simulations (Stiperski & Grubišić, 2011; SG11 hereafter) suggest that placing a **second mountain** the domain significantly alters the lee wave field.
- **Constructive or destructive interference** is determined by the mountain height ratio and the valley width.

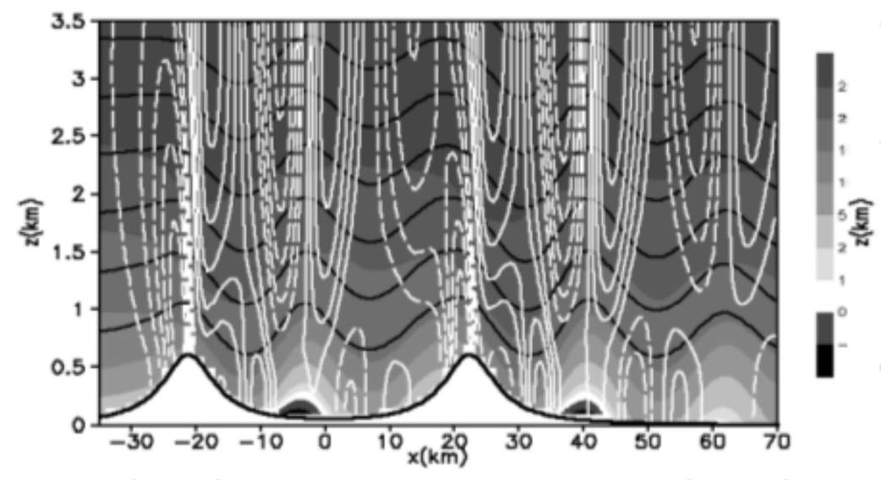

(fig 7) constructive interference (SG11)

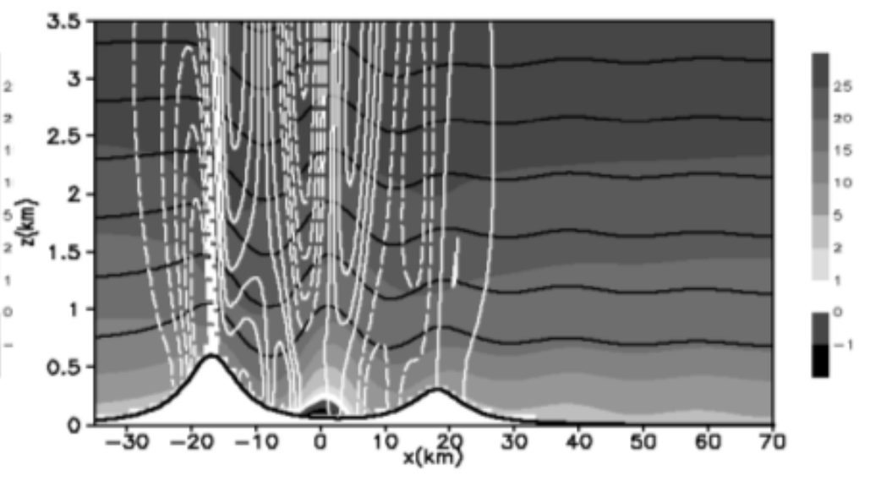

(fig 8) destructive interference (SG11)

**Non-dimensional parameters**
Mountain height ratio: $\mathbf{h_2/h_1}$
Amplitude ratio: $\mathbf{A_2/A_s}$, $\mathbf{A_2/A_1}$
Non-dimensional valley width: $\mathbf{V/\lambda_s}$

### Motivation

- **New laboratory experiments** are planned with secondary topography. Can the effects of a second mountain also be observed in the laboratory?
- What are the **sensitivities** of the flow field in a possible laboratory setup?
- How intense is the **turbulence** associated with rotors and hydraulic jumps?

## Numerical Simulations

- Model: **CM1** (Cloud Model 1) by George Bryan
- **Idealized simulations** both in 2D and 3D

- **Sensitivity tests (2D):**
  Test set 1 (STI): Sensitivities to changes in atmospheric sounding, terrain, bottom friction, and valley width
  Test set 2 (STII): Sensitivities on nonlinearity
- **3D simulations:** selected cases from STII.

dx=dy=50 m
Vertical grid stretching; high resolution (dz=10 m) on the ground and in the inversion layer.
Quasi-no-slip boundary condition
Topography: One or two Gaussian-shaped mountain(s), h=400 m (STI); h=1000 m (STII & 3D)
Input sounding: constant wind speed, strong inversion (fig 1)

## Sensitivity Tests (2D)

- **Lee wave interference test**: How does the valley width influence the interference pattern?
- The interference pattern of STI (fig 11) shows a **better agreement with the nonlinear interference pattern** (fig 10, blue line) of SG11 for mountains with h=1000 m.
- This is related to large-amplitude lee waves supported by the strong inversion and the related **nonlinear effects** in our simulations.

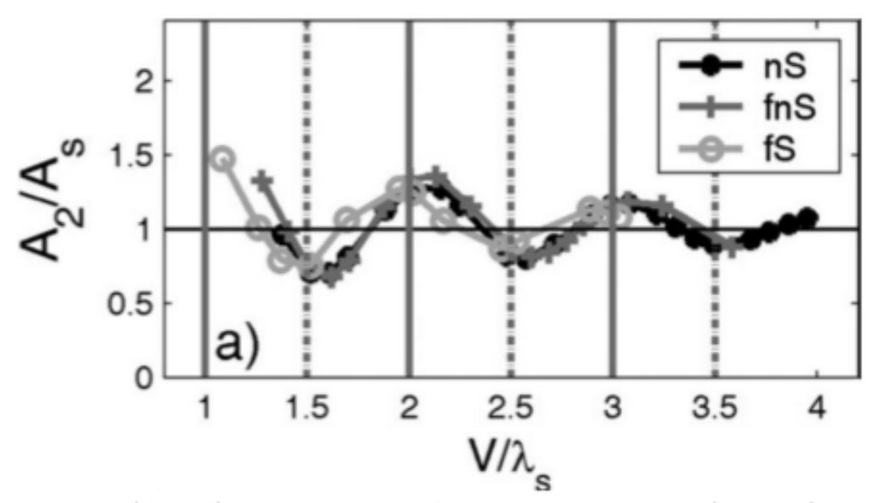

(fig 9) linear interference pattern (SG11)

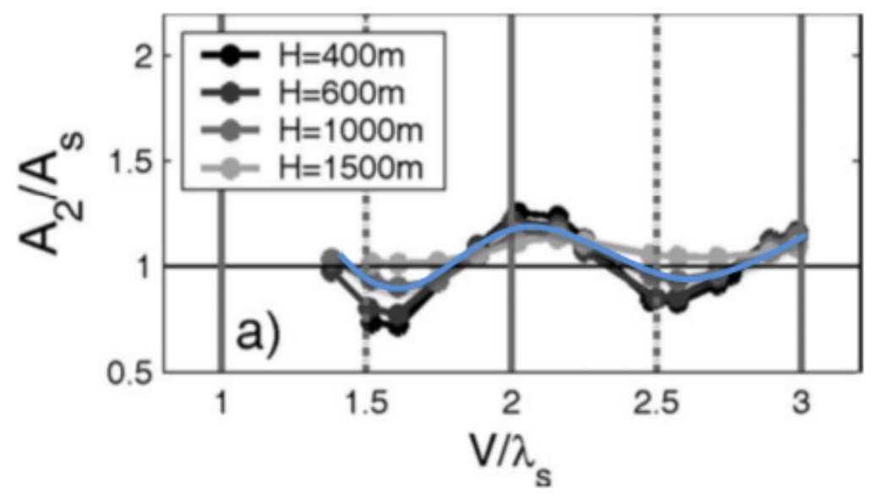

(fig 10) nonlinear interference pattern (SG11)

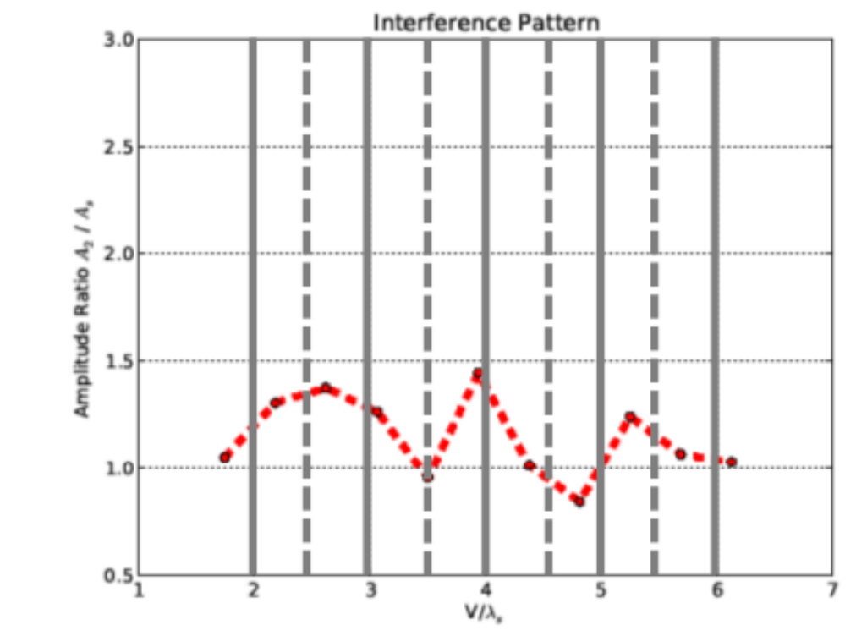

(fig 11) interference pattern of the sensitivity test with varying valley width.

### Influence of Secondary Topography

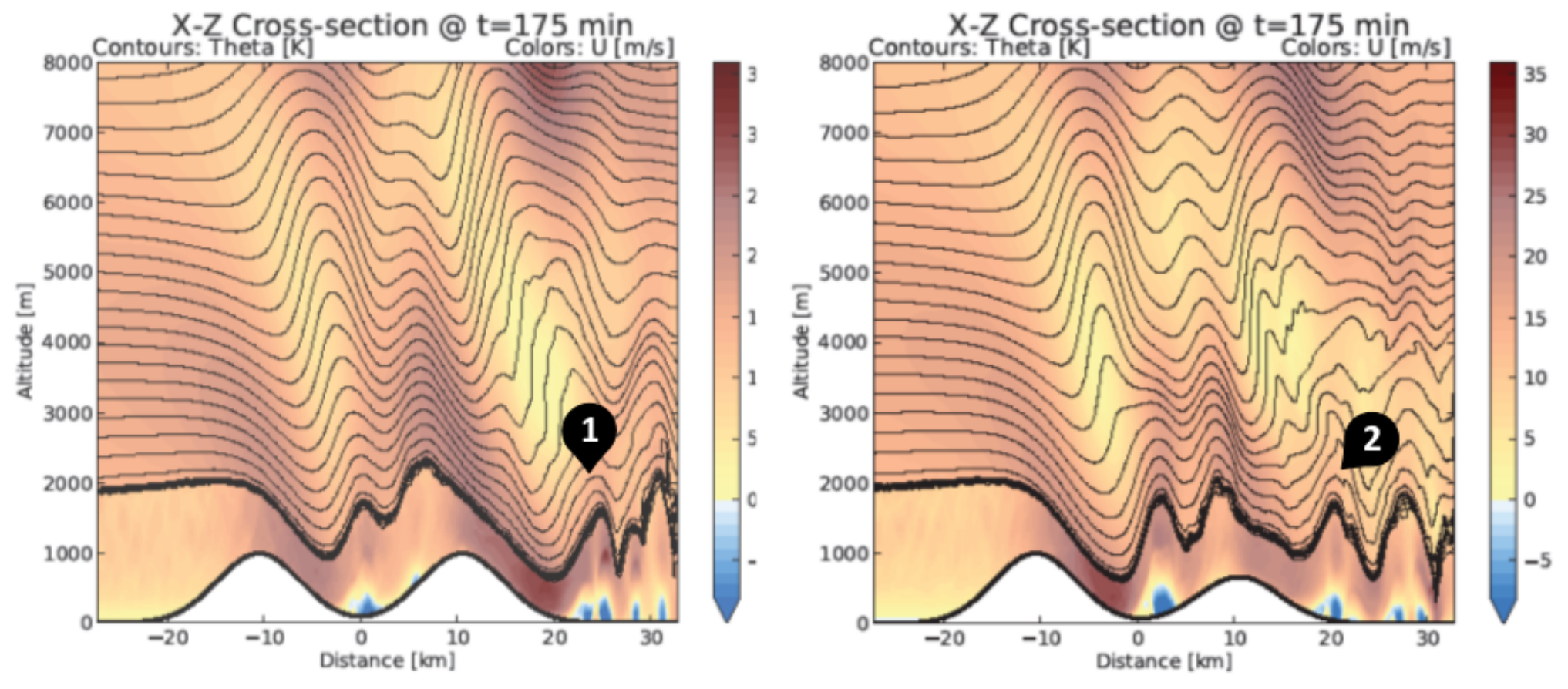

① **Constructive Interference.** The downslope windstorm and the lee wave amplitude in the lee of both mountains is enhanced. The mountain height ratio is 1.

② **Destructive interference.** The second mountain diminishes the lee wave amplitude behind both mountains significantly. The mountain height ratio is 2/3.

## Lee Wave Rotor (3D)

$Fr=0.7, h/z_i=0.6$

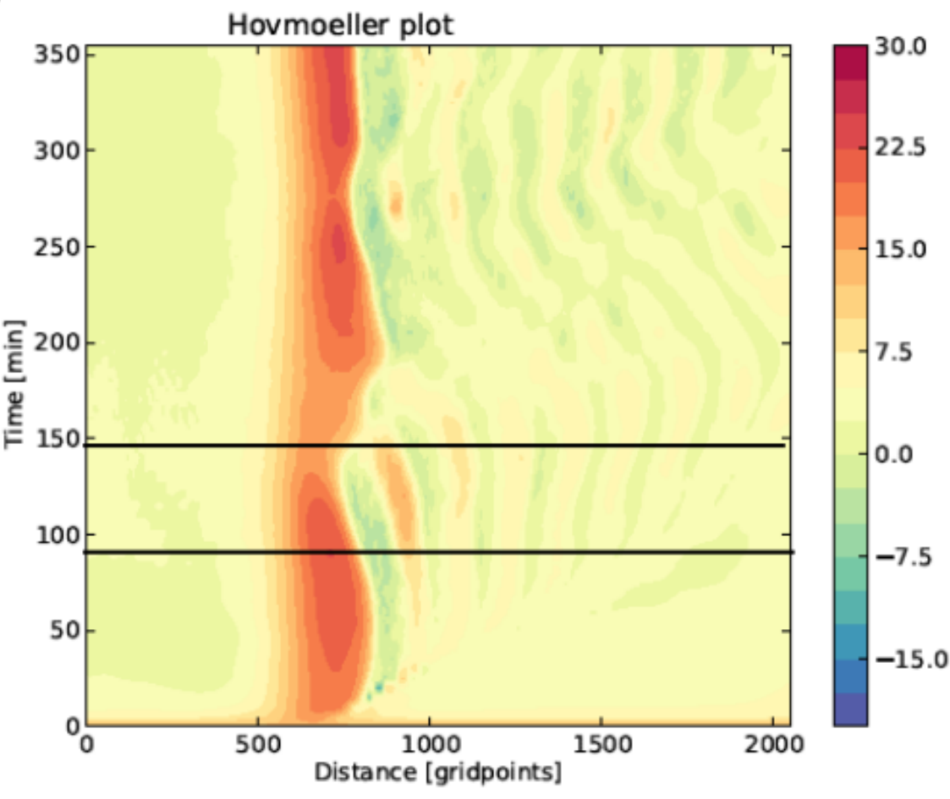

- Similar to the 2D equivalents, the 3D simulation is characterized by large-amplitude lee waves.
- The Hovmöller plot (lowest model level) shows the **unsteadiness of the flow** related to the breaking hydrostatic wave.
- Rotor formation and development is strongly **connected to the hydrostatic wave**.
- The following plots show the flow field at different times, indicated by black lines in the Hovmöller plot.

**u** The rotor below the lee wave crest is characterized by reverse flow (t=90 min). After the hydrostatic wave breaks and dissipates (t=145 min), the rotor flow is also significantly weakened.

**η** The horizontal vorticity field reveals that the rotor consists of several subrotors.

**TKE** The TKE maximum is located at the rotor updraft below the lee wave crest (t=90 min). When the rotor weakens (t=145 min), the turbulent kinetic energy is also reduced.

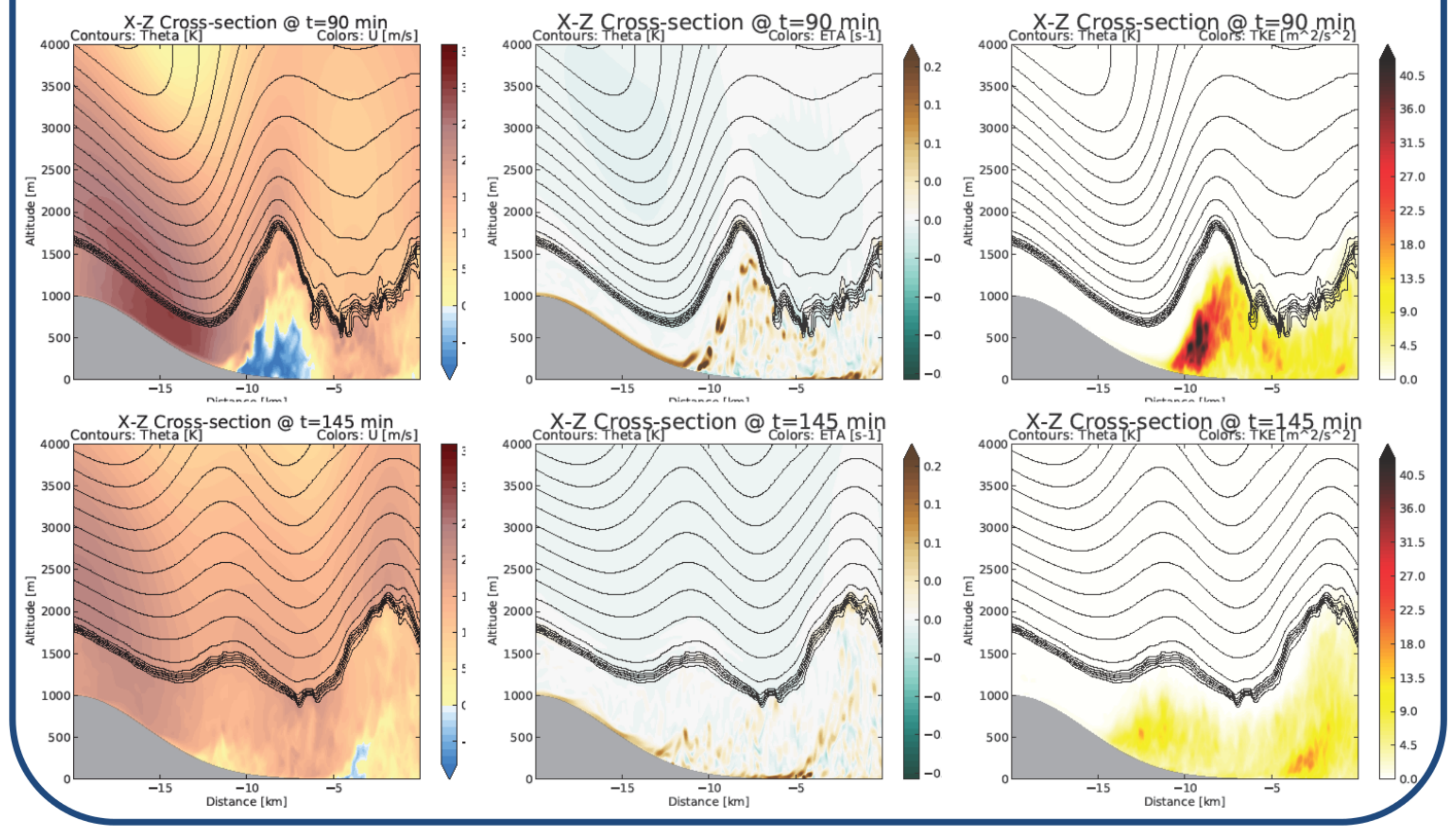

## Hydraulic Jump (3D)

$Fr=0.38, h/z_i=0.6$

- Simply changing the horizontal wind speed in the upstream sounding **transforms** a lee wave regime to a hydraulic jump regime.
- The hydrostatic wave in the hydraulic jump case is weaker.
- Hence, the simulation is more steady.
- However, when the hydrostatic wave breaks, it **merges together** with the jump and **enhances rotor strength and turbulence** intensity suddenly.

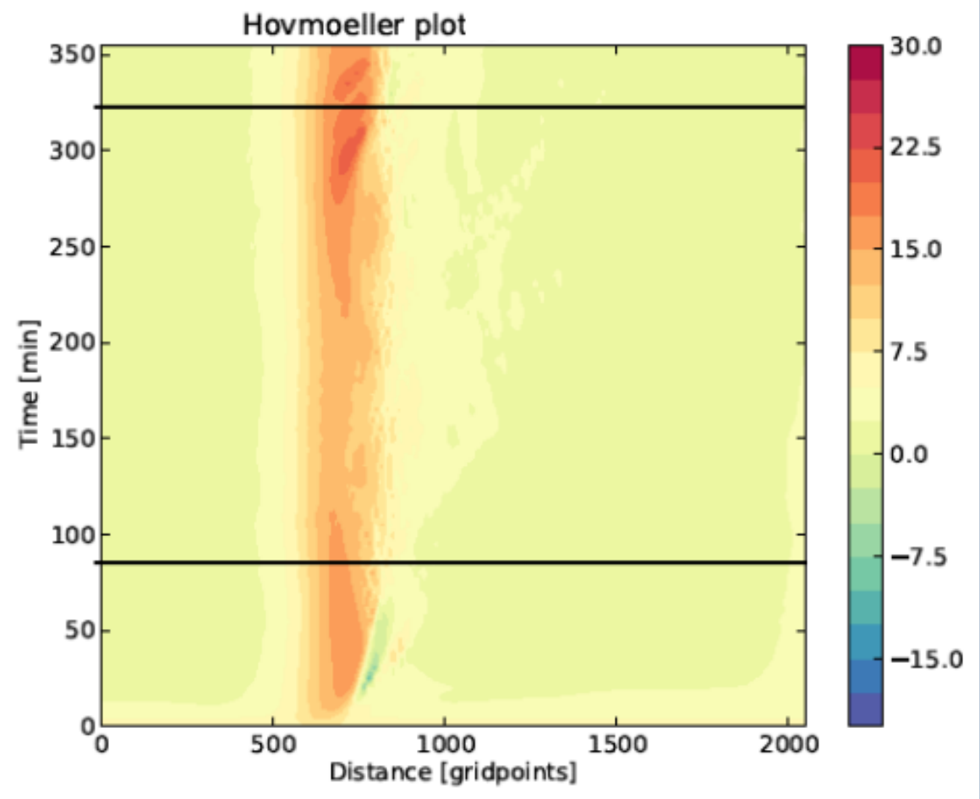

**u** The reverse flow within the jump region is weaker than in the lee wave rotor.
Wave breaking (t=315 min), however, leads to an increase in intensity.

**η** The most intense subrotors are observed when the breaking wave merges together with the hydraulic jump.

**TKE** Turbulence is weak during most of the simulation time. The breaking hydrostatic wave leads to a sudden increase in TKE throughout the whole domain (t=345 min).

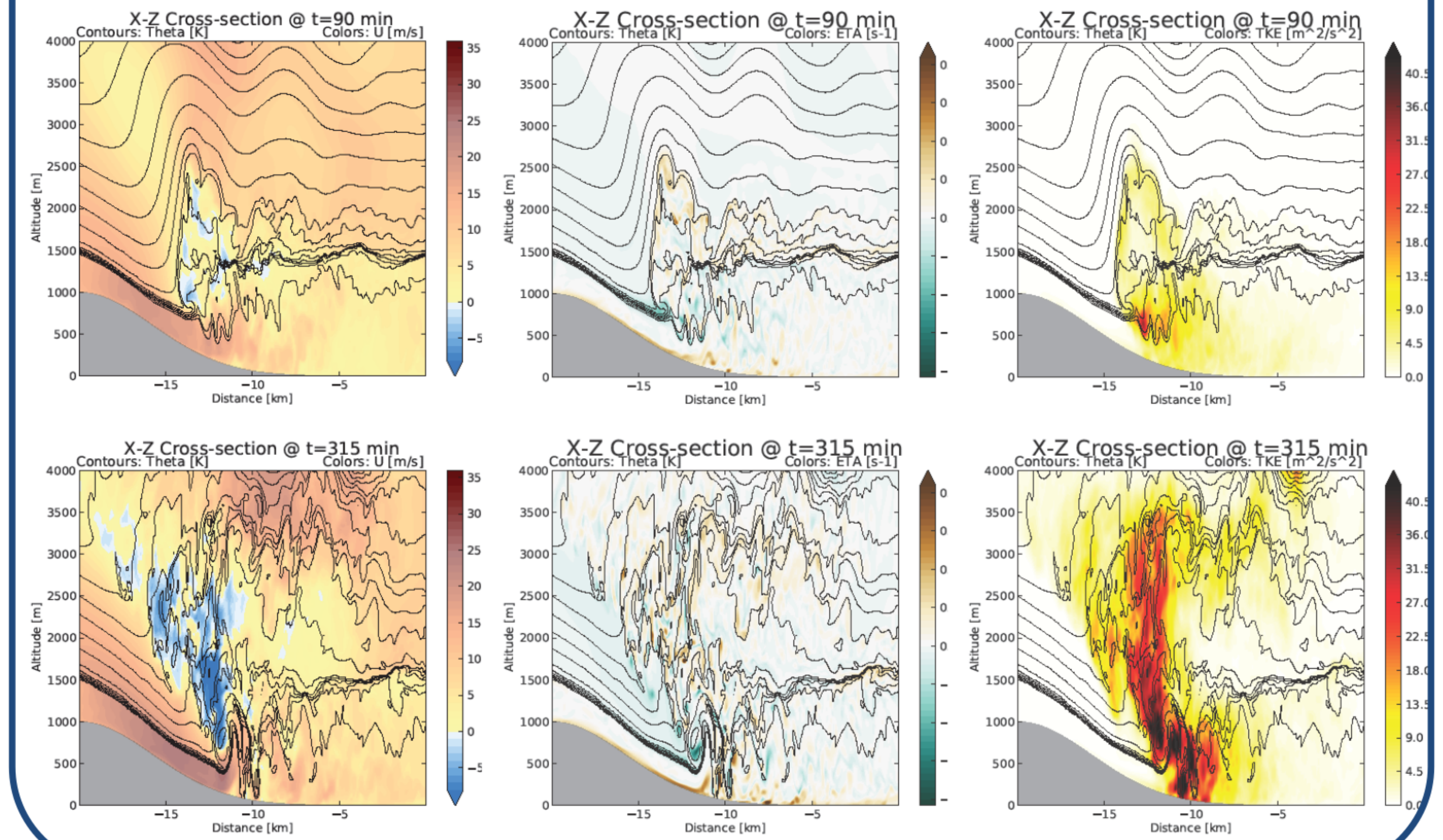

## Conclusions

- The 2D simulations show that nonlinearity plays an important role in the laboratory setup.
- The influence of the second mountain is still present, also in highly nonlinear regimes.
- Breaking hydrostatic waves lead to unsteady flow.
- Rotor strength and intensity are connected to the current state of the hydrostatic wave.
- Hydraulic jumps intensify extremely fast when the hydrostatic wave breaks, establishing a high-reaching turbulent zone.
- The simulations show that the phenomena of interest (effects of secondary topography, rotors, hydraulic jumps) can occur in a possible laboratory setup.

### References

- Vosper, S., 2004: Inversion effects on mountain lee waves. Q.J.R. Meteorol. Soc., 130, 1723–1748.
- Knigge, C., D. Etling, A. Paci, and O. Eiff, 2010: Laboratory experiments on mountain-induced rotors. Q. J. R. Meteorol. Soc., 136, 442–450.
- Stiperski, I. and V. Grubišić, 2011: Trapped lee wave interference in the presence of surface friction. J. Atmos. Sci., 68, 918-935.

Research partially supported by the Austrian Science Funds, FWF, through the project P 24726–N27 **STABLEST – Stable Boundary Layer Separation and Turbulence**

**Contact:**
**Brigitta Goger (brigitta.goger@uibk.ac.at)**
University of Innsbruck, Institute of Meteorology and Geophysics
Innrain 52f, 6020 Innsbruck, Austria